D33

N79-24034

MATERIALS AND TECHNIQUES FOR SPACECRAFT STATIC CHARGE CONTROL II*

R. E. Schmidt and A. E. Eagles
General Electric Company
Space Division

Results of exploratory development on the design, fabrication and testing of transparent conductive coatings, conductive bulk materials and grounding techniques for application to high resistivity spacecraft dielectric materials to obtain control of static charge buildup are presented.

Deposition techniques for application of indium oxide, indium/tin oxide and other metal oxide thin films on Kapton, FEP Teflon, OSR and solar cell coverglasses are discussed. The techniques include RF and Magnetron sputtering and vapor deposition. Development, fabrication and testing of conductive glass tiles for OSR and solar cell coverglass applications is discussed.

Several grounding techniques for rapid charge dissipation from the conductively coated polymer and glass dielectrics which have been developed and tested in thermal cycled and electron plasma environments are described.

Results of the optical and electrical characterization and aging effects of these coatings, bulk materials and grounding techniques are discussed as they apply to the performance of their design functions in a geosynchronous orbit environment.

INTRODUCTION

Passive temperature control of spacecraft equilibrium temperature is accomplished by a controlled mix of solar reflective and infrared emissive properties of the materials on the spacecraft's external surfaces. High dielectric insulating materials are commonly used for this passive control because of their high solar reflectance in second surface mirror configurations and inherent high emittance. This class of materials includes back surface aluminized Kapton films, silvered FEP Teflon films and high purity silica glass with a back surface silver coating for use as Optical Solar Reflectors (OSR's), all of which are used as thermal control materials.

In geosynchronous orbit these dielectric materials are directly exposed to high energy electron plasmas which are particularly severe during geomagnetic substorm activity. As high dielectric insulating materials these materials will collect and support electric charge buildup until the dielectric strength is exceeded and electrical discharge or arcing occurs to areas or components with lower potential energy. These discharges result

* This work was supported by the Air Force Materials Laboratory under Contracts F33615-76-C-5075 and F33615-76-C-5258.

in degradation of the thermo-optical and mechanical properties and interference with low level logic commands to and from the spacecraft due to the radio frequency noise generated by the arc. Furthermore, the degradation of the thermal control surfaces by vaporization of the material itself or their second surface metalized coatings may interfere with other sensor systems by condensation of these volatiles on detector or radiator surfaces.

The purpose of this paper is to describe the development of materials and techniques to prevent and/or control the electrostatic charge buildup on several materials most commonly found on the external surfaces of geosynchronous orbiting satellites. It represents the progress made during the last eighteen months of a materials development and test program on developing transparent conductive coatings and materials for application to dielectric materials including

(1) Uncoated and silvered FEP Teflon thin films (2-5 mil) used for solar reflecting second surface mirrors with high emittance for thermal control coatings

(2) Uncoated and aluminized (back surface) Kapton type H film (2-3 mil) commonly used as a top layer for multilayer insulation blankets

(3) Optical Solar Reflecting (OSR) tiles (typically 8 mil) of fused silica with a back surface coating of silver and Inconel for second surface mirror applications requiring high thermal emittance surfaces (similar to the performance of the silvered FEP Teflon coating)

(4) Glass slides of fused silica and borosilicate (or microsheet) which are used for cover slides on silicon solar cells

APPROACH TO THE PROBLEM

Transparent Conductive Coatings

Conductive transparent coatings from semiconductor - metal oxides represent one possible means of controlling electrostatic charge buildup while having a minimal effect on the α and ϵ properties of the spacecraft materials. The most commonly used thin oxide films for transparent and conductive coatings have been combinations of indium oxide and tin oxide. The conductivity of these oxide coatings, first developed as resistance heaters on glass surfaces, is critically dependent on the creation of a proper oxygen-metal balance during the deposition to provide sufficient conduction electrons in the coating. The properties of these and other metal oxide coatings have been found to be strongly dependent on the conditions of the substrate and the deposition process.

Thin films of 90% indium oxide and 10% tin oxide have been deposited

onto 3 mil Kapton, 5 mil FEP Teflon sheets and OSR and coverglass tiles of fused silica and borosilicate using Magnetron, DC and RF sputtering and resistive heating vapor deposition techniques. Deposition has been demonstrated both reactively by Magnetron and DC sputtering and by resistive heating from In/Sn metal targets in an oxygen and argon atmosphere and non-reactively by RF sputtering from a dielectric indium/tin oxide target.

Visible absorptance and infrared emittance measurements of indium-tin oxide (ITO) reactively sputtered onto FEP Teflon films as conductive coatings in thicknesses up to 900 Å show a definite dependence upon thickness. Emittance, solar absorptance and transmittance in the visible region are shown in Figure 1 as a function of the coating thickness. As shown, the effect of the coating thickness is more pronounced in the visible spectrum than in the infrared.

Indium oxide and aluminum oxide coatings have been deposited in thicknesses down to 100 Å by resistive heating vapor deposition onto FEP Teflon and Kapton films and microsheet tiles. The films that were formed after the deposition were slightly dark due to oxygen deficiencies in the coatings. However, after heating in air at about 220°C for a period of 15 minutes the coatings were highly transparent with sheet resistances in the 10^8 ohm/square range. The results of these coatings are shown in Table I. Optical measurements between 0.27 and 2.7 μm show that heat treating at 200°C had no affect on the transmission of the Teflon film.

Reproduction of conductive transparent coatings was found to be strongly dependent upon the deposition technique and preparation parameters such as substrate temperature, vacuum, background of carrier gas and ratio of carrier to reactive gas, power levels and geometry of sample to source. Heat treatment of the coatings following the deposition as described above in some instances was found necessary to improve the transmittance of the thin film coatings. Table 2 shows some of the control variables which have been considered in depositing ITO by Magnetron sputtering.

The effect of post deposition heat treatment in air is most evident as a marked improvement in the optical transmission of the films deposited in both reactive and non-reactive deposition techniques. It has been found that the addition of an RF field to the planetary fixture during the magnetron sputtering relieves the requirements for this post-deposition heat treatment. The additional RF activation was found to have its most pronounced effect on the optical and electrical properties of the film when used during the deposition, while use following the deposition seemed to have little to no effect.

Other oxides of antimony, bismuth, lead, zinc, cadmium, titanium and silicon were also evaluated using resistive heating vapor deposition. All of the oxides showed reasonably high transmission on microsheet after post-deposition heat treatment but in general, showed high resistance insulator qualities or had surface resistances which varied considerably from batch to batch.

In general, most conductive and reproducible transparent coatings

were produced reactively by magnetron sputtering of indium-tin oxide from a 90% indium/10% tin target in a closely controlled oxygen/argon atmosphere with an in situ RF field applied to the planetary. The resulting ITO coatings had surface resistances predominantly in the low kilohms/square range in addition to a very low change in the absorptance of the substrate. Figure 2 shows a typical spectral response curve for 300 Å coating on a 5 mil FEP Teflon film and 10 mil borosilicate substrate.

Conductive Glass Development

A lithium borosilicate glass developed by GE several years ago under AFML contract F 33615-71-C-1656 with the designation GE-1TL was considered as a substitute glass material to prevent static charge buildup because of its good transmission and resistance to high energy electron (beta) radiation. A solid 11.4 cm diameter sample of the modified lithium borosilicate glass was cast in a shallow graphite mold, annealed and finally polished to a 0.14 cm (55 mil) thickness. A comparison of the transmittance of this glass with fused silica and borosilicate is shown in Figure 3A. A 1" x 1" x 1.8" block of the lithium borosilicate glass shown in Figure 3b was poured, annealed, cut and polished into 1" square wafers about 0.25 mm (10 mil) thick. These slides were then coated on one side with a 0.2 μm coating of silver to simulate an actual OSR configuration. Figure 3c is a plot of the solar reflectance and thermal emittance at 100°F of the GE 1TL glass tiles. The spectral weighted average of these curves give a value of R = 0.88 and α = 0.12 with ϵ = 0.86. Bulk resistance measurements of the 0.14 cm (55 mil) thick glass according to ASTM-D257 showed the modified lithium borosilicate resistance to be of the order of 10^{11} ohms.

Conductive Adhesive

Optical Solar Reflectors (OSR's) of fused silica and borosilicate (Corning 0211 microsheet) tiles have been coated with indium oxide, indium tin oxide and other metal oxides for evaluation during this program. Typically, three inch square matrices of one inch and three quarter inch square tiles have been mounted to aluminum plates as shown in Figure 4a for testing. A conductive, low outgassing, graphite loaded adhesive has been developed to bond the OSR's and provide a conductive path for charge dissipation to the spacecraft structure. The adhesive composition consisted of RTV 566 or 560 filled with 13% by weight of Hercules ¼ mm chopped graphite fibers. The RTV 566/HMS fiber formulation produced a resistivity of about 7.5×10^4 ohm-cm. The conductive adhesive in combination with the ITO or IO coated OSR's as shown in Figure 4b has been shown to provide a space stable adhesive system which provides a reliable conductive path between the coating and the metal support surface.

Chamfering

A major concern in using conductive coatings on OSR's and solar cell coverglasses is achieving a durable and continuous coating around the front

surface to the sides of the glass for a conductive path to the metal support structure. Chamfering of the glass edges in order to deposit a reliable hard and continuous conductive coating on the front and sides of the glass coupon was demonstrated as an alternate to the currently used method of welding conductive leads to contact points on each tile. The capillary action of the conductive adhesive between the tiles when they are pressed into position then provided the necessary conductive link between the coating and the metal frame, as illustrated in Figure 4c. Glass tiles of fused silica and microsheet have been successfully chamfered at a 45^{o} angle using 600 grit emory polishing paper, as shown in Figure 5a under 3X magnification where each division is 0.127 mm (5 mils). A final OSR configuration with ITO coated chamfered 2 cm square microsheet tiles is shown in Figure 5b.

Solar Cell Coverglasses

Active solar cells in typically 2 cm by 4 cm size were used in fabricating, testing and evaluating the conductive transparent coatings and grounding techniques. Coverglasses of fused silica, microsheet and Cerium doped microsheet were bonded to the solar cells using Sylgard 182 or RTV 142. Typically, arrays were fabricated for testing in two series sets of 4 parallel cells as shown in Figure 6. The solar cells were then bonded to 3 mil Kapton substrates with Sylgard 182 and then mounted to an aluminum plate. Resistance measurements between the transparent conductively coated coverglasses and the solar cell circuit after mounting showed a high resistance of the order of 10^{11} ohms on a majority of the coated coverglasses. This high resistance is a result of the lack of a reliable conductive path between the coverglass coating and the solar cell bus electrode. Coating the coverglass after it had been mounted to the solar cell did not significantly improve the probability of creating a conductive path between the top of the coverglass the solar cell electrode. To improve the conductivity of this charge leakage path a silver loaded epoxy 1109S from Electroscience Labs was applied to the junction of the coverglass and solar cell bus electrode as shown in Figure 7a. After applying this conductive epoxy diluted with 3:1 mixture of Xylene along the edge of the glass and curing in air at 100^{o} C for 90 minutes, the resistance between the solar cell electrode and the IO coated coverglasses, as shown in Figure 7b, was reduced to the order of 10^{5} ohms for all the coverglasses.

Ground Bond Development

Several grounding techniques were evaluated to provide connections between conductive coatings on the Kapton and FEP Teflon films and the spacecraft structure. The objective was to provide integral metal to polymer film laminates with high peel and shear strengths which could withstand the thermal and electrical cycling environment of geosynchronous orbit. Four design configurations evaluated were

1. Adhesive bonded metal to polymer and overcoated with conductive oxide

2. Heat sealed metal to polymer bonds

3. Adhesive bonded metal to conductively coated polymer

4. Mechanical clamp to the conductively coated polymer

One mil thick thermo setting DuPont Pyralux adhesive was used to bond 1 mil thick copper foil to coated and uncoated substrates of 3 mil Kapton. The composite shown in figure 8a was formed between two heated plates (175°C) under about 1.34 x 10^6 Pascals (200 psi) for 2 minutes. A 500 Å coating of indium oxide over the entire Kapton sample including the ground tab provided a solderable joint with a resistance of 10^7 ohms to anywhere on the film surface. No success was obtained in trying to bond copper foil directly to the FEP Teflon using the Pyralux adhesive without any surface treatment. A direct heat sealing of the copper foil to the FEP Teflon was also attempted. However, the heat required to bond the FEP to the copper foil resulted in severe surface distortion and the Teflon to foil sealing edge was very susceptible to cracking. Application of an etching solution of Tetra Etch to the FEP Teflon improved the surface adhesion so that application of Pyralux sheet adhesive and copper foil as described above provided a strong solderable bond.

Adhesive bonding of the grounding electrode to the conductive oxide coated polymer films was also evaluated. Conductive tapes and epoxies were considered for application to the ITO coated polymers for attaching a solderable metal foil to the conductive coating. Table 3 summarizes the various ground bond configurations tested. For this application 3M's conductive copper tape X1181 showed much greater adhesion to the ITO coated Teflon and Kapton films than Eccobond's silver loaded epoxy. It was found that application of the Pyralux to the coated FEP surface required etching the coating from the FEP before a strong adhesive bond could be obtained. Thermal cycling tests were performed in air between -65° and +100°C on these bonds to evaluate their stability. Resistance measurements between the ground tabs and the ITO coatings during the thermal cycling are summarized in Table 4. The variation in a typical run is illustrated in Figure 9. These test results indicate that all the configurations were electrically stable during the three cycle test.

STATIC CHARGE TESTING

Test Facility

The electrostatic charging and control facility is shown schematically in Figure 10. The facility is designed to irradiate flat samples up to 4.5 inches in diameter at electron energies up to 30 KeV in a vacuum system which is initially in the mid 10^{-7} Torr range. The design of the gun includes a three element electrostatic lens to obtain uniform beam density across the sample area and allow adjustment in flux density. Current measuring electrodes are connected to the rear of the aluminum back plate sample holder for bulk leakage currents and to the annular sample retaining ring for surface leakage current monitoring.

A secondary electron collector cylinder is also part of the system which can be swung in place around the sample during irradiation to monitor charged particles leaving the surface of the sample. A Monroe model 144-1009s non-contacting electrostatic voltmeter probe is mounted on a rotable arm which can be swept across the sample surface when the secondary cylinder is not in place. During irradiation the probe may be swung completely out of the way of the beam or may be used to measure surface potentials during irradiation.

Coating Charge Control

Indium oxide (IO) and indium tin oxide conductively coated FEP Teflon and Kapton films were tested in the charging control facility. Bulk (I_D) and surface (I_R) conduction currents were recorded for beam potentials between 2KV and 20KV for the first several minutes of irradiation and also following shut off of the electron beam. Initial maxima and steady state values for the IO and ITO coated 3 mil Kapton and 5 mil FEP Teflon are shown in Tables 5 and 6. Surface potential measurements using the Monroe electrostatic voltmeter following irradiation at beam potentials of 10KV, 15KV and 20KV showed surface potentials of less than 5 volts for all four materials tested.

The typical line shape of the conduction currents I_D and I_R as the electron beam was turned on and off for the Kapton and Teflon materials is shown in Figure 11. Integration of the current over the transient portion of the current curves show that most of the charge deposited in the film below the coating was quickly dissipated when the beam was turned off as shown in Table 7.

Electron irradiation tests were also conducted on the ITO coated Kapton and Teflon samples for several hours over a period of six months. Between these tests the samples were stored in a dust free environment at room temperature. Following this series of tests no visible sample degradation was observed and the surface resistance measurements on the sample were in the $4\text{-}10\times10^6$ ohm/square range before and after the irradiations.

Ground Bond Tests

The copper foil grounding connection on Kapton using Pyralux adhesive and overcoated with conductive transparent indium oxide, shown in Figure 8 was tested under electron irradiation. The surface current electrode was isolated from the perimeter of the sample except at the ground tab. The bulk and surface leakage currents were similar in character to those reported in Table 6.

Ground bonds soldered to conductive copper tape or copper tab/conductive epoxy and bonded to ITO coated films of Teflon and Kapton were also irradiated by 2KeV to 20KeV electrons. Figures 12a and 12b shows the general test configuration for the two bonding methods. Figure 12c shows the detail of the copper tab/Eccobond 56C/ITO ground connector on the Teflon. Bulk, surface and secondary collector currents were similar to those reported above. However, surface potentials up to -100V were

measured on samples shown in Figures 12b and c when irradiated at 20KV. These surface potentials were centered around the solder joints on the ground tabs and examination after the test revealed that traces of solder flux on the leads was responsible for the small charge accumulation.

OSR Matrix Testing

Table 8 shows a summary of the OSR configurations tested under electron irradiation. The effective conductivity or charge control of the graphite loaded RTV 566 was measured under electron irradiation to provide a baseline for future OSR matrix tests using the conductive adhesive. Table 9 summarizes the measured currents through the material (I_p) and the secondary electron collector. The surface potentials measured following irradiation show that the material charged nominally to between -90 and -160 volts.

Uncoated OSR Matrix

A three inch square matrix of nine square tiles of fused silica without any conductive coating was exposed to monoenergetic electron beams between 2KeV and 20KeV at nearly 10nA/cm^2 for several minutes. The glasses were mounted using the conductive adhesive. Currents measured through the backplate, around the perimeter and from the secondary collector are shown in Table 10. The maximum surface potential exceeded the range of the Monroe voltmeter following irradiation in a 4KeV beam but did not show electrostatic discharging until irradiated in a 15KeV beam. Reducing the beam density to below 4nA/cm^2 reduced the discharge rate but not proportionally. A similar set of measurements and observations were made on a 3 inch square matrix of uncoated OSR tiles of microsheet. Similar currents and potentials were also measured on an OSR matrix covering the entire 4.5" diameter sample area. Decay of the surface potential following irradiation at 6KV followed an exponential decay very closely with a 12.5 minute time constant and an initial potential of about -2100 volts.

An uncoated three inch square matrix of 16 chamfered 10 mil thick microsheet tiles using the conductive RTV was also tested under electron bombardment. Although similar current and surface potentials were measured as before for the other uncoated tiles and discharging was observed during the 15KeV beam irradiation, the discharge rates were not as regular as before. Figure 13 shows the variation of surface potential with electron beam energy for this uncoated OSR up to 6KeV irradiation.

Conductively Coated OSR Matrices

An OSR mosaic of 16 ITO coated 2 cm microsheet tiles mounted with conductive adhesive to an aluminum plate was irradiated in an electron beam with energies up to 20 KeV. The peak and steady state bulk leakage and secondary collector currents are listed in Table 11. Note that in contrast to the uncoated sample currents, the initial peak is much smaller, indicating a much smaller subsurface charge deposit than in the uncoated materials. Surface potential measurements with the capacitively coupled probe gave maximum surface voltages of 37V, 46V, and 45V after

irradiation by 10KeV, 15KeV and 20KeV electrons, respectively.

A 16 tile matrix of ITO coated chamfered 2 cm square microsheet tiles with conductive adhesive bonding was also tested. The test results, shown in Table 12, indicate the successful charge control demonstrated by the coated tiles. Measurement of the negligible surface potential and the lack of a subsurface charging peak on the bulk leakage current indicate a negligible charge buildup on this sample.

Conductive Glass OSR

Electron irradiation tests on a 3 inch square matrix of 0.38 mm (15 mil) thick one inch square tiles of modified lithium borosilicate (GE-iTL) glass with a silvered back surface between beam energies of 2 to 20 KeV showed no significant charge buildup on the glass surface. Bulk leakage and secondary collector currents are given in Table 13 for an average beam density of about 10nA/cm^2. No surface electrode was used on these samples because the relative conductance of the glass prevented any surface charge buildup.

Solar Cell Arrays

Four solar cell arrays were tested under irradiation by electron plasmas with energies up to 20 KeV. They were fabricated with varying degrees of charge control solutions. All of the arrays tested were fabricated in an active 2 cell by 4 cell arrangement with two series sets of 4 parallel cells. The two cm by four cm cell array thus formed a 7.6 cm (3 inch) square array. The array was tested in an active mode with a 10 ohm load resistor across the array leads. A beam aperture adaptor with a three-inch diameter similar to the one used for testing the OSR matrices was attached to the secondary collector approximately one-inch in front of the test fixture in order to restrict the electron beam to the solar cell area of the sample test fixture.

The initial configuration tested was an uncoated array. Unusually low potentials were recorded at all beam energies and no severe discharging was observed. Surface potentials of 360V, 830V, 1KV and 1.2KV were recorded after exposure to beam energies of 5, 10, 15 and 20KeV respectively. The low surface potentials for this uncoated sample was attributed to the small current output of the electron gun of about 0.2nA/cm^2 during this set of measurements.

An array was next tested whose coverglasses had been coated with indium oxide. The first set of measurements were made on the coated solar array without any conductive epoxy applied to the coverglass/solar cell bus area. Measurements were terminated after observing severe discharging while being irradiated in a 5KeV beam with a current density of 5nA/cm^2. The arcing and discharging disappeared after the solar cell bus/coverglass junction was overlaid with a coating of Electroscience 1109S conductive epoxy and retested in an electron

beam at energies up to 20KeV with beam densities up to 5nA/cm^2.

The next cell array tested used IO coated chamfered coverglasses with conductive epoxy applied along the chamfered edge and the cell electrode. Low surface potentials of 170, 275, 335, 365 and 390V at 4, 6, 10, 15 and 20KeV beam potentials indicate that no significant charge build up was occurring on the solar cell coverglasses. The IV performance of this array, before and after the irradiation is shown in Figure 14 and indicates a slight decrease in the power output of the cell. However the same magnitude decrease in power output was also observed on the uncoated array after electron irradiation.

A four by two solar cell array with Cerium doped microsheet coverglasses from Pelkington P.E. (PPE) was also tested in the ESD facility with energies up to 10KeV. The surface potentials measured with the Monoroe probe were nearly up to -2000V after irradiation in a 6KeV beam in contrast to the low potentials measured on the IO coated coverglasses. Due to high surface charge accumulation on the cerium doped coverglasses it is evident that the doping is insufficient to control the electrostatic charge buildup and further tests were terminated in order not to destroy the cells. The same type of decrease in power output was observed in these cells, shown in Figure 15, as was observed in the coated cell as a result of the irradiation tests.

Electron/UV Exposure

Six Teflon sample configurations were exposed to 1000 hours of combined electrons and the equivalent of one UV sun. The 5 mil thick samples which were tested were 1) Virgin FEP Teflon; 2) FEP Teflon which had been heat treated at 200°C for 30 minutes; 3) FEP Teflon with a 200 MΩ conductive coating of indium oxide which had been heat treated as in No. 2 and, 4-6) three samples with conductive coatings of indium oxide of different thicknesses and a thin flash overcoating of chrome oxide. The IO and chrome oxide coatings were deposited with the resistance heating at $1x10^{-4}$ Torr O_2 partial pressure. The indium was deposited in thicknesses of 350, 500, and 750 Å. Table 14 summarizes the average transmittance weighted over the solar spectrum from measurements in air before and after the exposure. Addition of the flash coating of the chromium oxide seems to retard the degradation of the coating.

CONCLUSION

Thin films of indium oxide and indium tin oxide have been successfully and reproducibly deposited as conductive transparent coatings onto glass, Kapton and FEP Teflon sheets as large as one foot square. Deposition by Magnetron sputtering has produced the most consistent and uniform coatings with no need for post deposition heat treatment resulting in coatings typically with a $\Delta\alpha$ of 0.02 from the uncoated substrates.

A modified lithium borosilicate glass developed by GE under another program has been fabricated in 0.38 mm (15 mil) OSR tiles. Tests under a simulated substorm environment have shown its ability to dissipate the incident charge flux and prevent any charge accumulation. The effective conductivity of the OSR bonding adhesive has been increased by the addition of graphite fiber to provide a conductive path between the transparent conductive coated OSR or conductive glass and the spacecraft grounding structure. The chamfering of the OSR tiles has been demonstrated along with the conductive coatings to provide a highly reliable conductive path from the front surface to the conductive adhesive.

Several grounding techniques have been evaluated for their ability to drain the charge buildup from the conductively coated surfaces of Teflon and Kapton films. The bonds have been thermally cycled and tested under electron irradiation in a simulated environment and have been shown to provide a stable conductive path between the conductive coating and spacecraft ground.

These conductive coatings, materials, and grounding techniques are now being further evaluated to determine the best coating thickness and processing techniques to provide the minimum optical interference to the substrate and still have a charge control material. Further development will evaluate the scale up of these processes for large samples and their behavior in larger and combined environments.

Table 1. Summary of Vacuum Vapor Deposited Transparent Conductive Oxide Films

MATERIAL	DEPOSITION RATE	BACKGROUND OXYGEN PRESSURE	TAPE (2) TEST	HEAT AT 425°F/ 15 MIN.	TRANSPARENCY	SURFACE RESISTIVITY (3) Ω/□	SUBSTRATE
Al_2O_3	25A/MIN.	5×10^{-5} TORR	P(1)	YES	NO DETECTABLE INCREASE IN TRANSMISSION BEFORE AND AFTER TESTING	5×10^{7} TO 5×10^{8}	KAPTON
In_2O_3	25A/MIN.	1×10^{-4} TORR	P	YES		5×10^{7} TO 5×10^{8}	KAPTON
In_2O_3	25A/MIN.	1×10^{-4} TORR	P	YES		5×10^{7} TO 5×10^{8}	FEP
Al_2O_3	250Å/MIN	5×10^{-5} TORR	P	YES		5×10^{7} TO 5×10^{8}	MICROSHEET
In_2O_3	250Å/MIN	1×10^{-4} TORR	P	YES		5×10^{7} TO 5×10^{8}	MICROSHEET
In_2O_3	250Å/MIN.	1×10^{-4} TORR	P	YES		5×10^{7} TO 5×10^{-8}	MICROSHEET

Table 2. Magnetron Coated FEP and Kapton

Material	Run	O_2 Partial Pressure Torr	Process Temp (°C)	Evaporation Rate Å/MIN	Thickness Å	Surface Resistivity Ω/□	Δ Transmission %
Kapton	24	3.8×10^{-4}	121	22	100	37K	.03
Kapton	25	4.4×10^{-4}	150	16	100	7.9K	.05
FEP	25	4.4×10^{-4}	150	16	100	7.9K	.10
Kapton	26	5.5×10^{-4}	121	2*	100	5×10^{8}	0
FEP	26	5.5×10^{-4}	121	2*	100	∞	0
Kapton	27	3.5×10^{-4}	100	20	300	12.5K	.10
FEP	27	3.5×10^{-4}	100	20	300	6.5K**	.16
Kapton	28	6×10^{-4}	100	22	300	350	.07
FEP	28	6×10^{-4}	100	22	300	1300	.10
FEP	28	6×10^{-4}	100	22	300	15000	.10
Kapton	29	4.9×10^{-4}	100	10	300	75K	.02

* Slow rate of evaporation enables more complete oxidation of ITO; increasing resistance and insulating properties of film.

** Post bake at 368°F for 4 hours reduced surface resistance to 1300 Ω/□.

Table 3. Copper Ground Bond Adhesion Strength

Substrate	Coating	Coating Etch	Substrate Etch	Adhesive	Shear Strength (psi)	Peel Strength (oz/in)
FEP Tefon	None		None	Pyralux	N/A	N/A
"	"		"	EA956*	5.6	N/A
"	"		"	Cu tape**	1.8	6.8
"	"		Tetra Etch	Pyralux	18.4	>32.0[a]
"	"		"	EA956	18.6	9.6
"	"		"	Cu tape	>21.6	36.0
"	ITO	None	None	Pyralux	18.6	8.3
"	"	"	"	EA956	19.2	7.7
"	"	"	"	56C	18.2	3.8
"	"	"	"	Cu tape	18.0	38.4
"	"	10% HCl	Tetra Etch	Pyralux	17.0	16.0
"	"	"	"	EA956	18.6	10.9
"	"	10% H_2SO_4	"	Pyralux	19.0	21.1
"	"	"	"	EA956	17.8	12.8
"	"	10% NH_4F HF	"	Pyralux	18.2	8.3
"	"	"	"	EA956	19.6	11.5
Kapton	None		None	Pyralux	84.0	115.2
"	"		"	EA956	95[a]	11.2
"	"		"	Cu tape	59.0	46.4
"	ITO	None	"	Pyralux	91.0	120.0
"	"	"	"	EA956	80.0	16.0
"	"	"	"	56C	40.0	11.2
"	"	"	"	Cu tape	56.0	35.2
"	"	10% HCl	"	Pyralux	93.0	144.0
"	"	"	"	EA956	84[a]	3.2
"	"	10% H_2SO_4	"	Pyralux	95[a]	a
"	"	"	"	EA956	87[a]	6.4
"	"	10% NH_4F HF	"	Pyralux	>100	128.0
"	"	"	"	EA956	72[a]	4.8
Aluminum	None	None	"	Cu tape	57	94.4

N/A - no measurable adhesion
a - substrate tore
* - Hysol adhesive EA956
** - 3M brand conductive tape #1181

Table 4. Extreme Values of Surface Resistance During Thermal Cycle Tests

Configuration	Minimum Resistance (10^5 Ω)	Maximum Resistance (10^5 Ω)
Copper Tape on ITO FEP Teflon	0.240	1.57
Copper Tape on ITO Kapton	0.114	0.472
Mechanical Clamp on ITO Kapton	0.032	0.078
Mechanical Clamp on ITO FEP Teflon	0.285	3.64
Copper Tab/EA 956/ITO Kapton	0.036	0.040
Copper Tab/Pyrolux/ITO Kapton	0.033	0.037
Copper Tab/56C/ITO FEP Teflon	0.645	1.52
Copper Tab/56C/ITO Kapton	0.133	0.257

Table 5. Summary of Current Measurements of IO and ITO FEP Teflon[a]

	IO FEP Teflon (Sample No. 44)					ITO FEP Teflon (Sample No. 37)				
Beam Potential (kV)	I_D[c] Max.	I_D S. S.[b]	I_R Max.	I_R S. S.	I_S S. S.	I_D Max.	I_D S. S.[b]	I_R Max.	I_R S. S.	I_S S. S.
2	0.05	0.03	11	11	180	0.8	0.05	99	26	240
6	0.1	0.02	220	150	90	2.2	0.05	270	150	125
10	0.25	0.02	360	200	75	2.6	0.05	280	200	90
15	0.4	0.02	300	200	55	3.5	0.05	450	310	99
20	0.65	0.02	300	200	45	4.5	0.05	470	340	85

[a] All currents in units of nanoamperes

[b] Steady State

[c] I_D bulk conduction current

I_R surface conduction current

I_S secondary collector current

Table 6. Summary of Current Measurements of IO and ITO KAPTON[a]

Beam Potential (kV)	IO-Kapton (Sample No. 40)					ITO-Kapton (Sample No. 36)				
	I_D[b]		I_R		I_S	I_D		I_R		I_S
	Max	S.S.[d]	Max	S.S.	S.S.[c]	Max	S.S.	Max	S.S.	S.S.
2	0.2		150	120	280	nm[d]	nm	nm	nm	nm
6	1.4	0.03	540	330	100	21	0.1	630	420	160
10	3.4	nm	570	340	90	4.3	0.05	630	450	nm
15	8.1	0.02	600	360	70	9.9	0.05	750	460	nm
20	12.6	0.02	500	360	60	6.0	0.05	690	570	nm

[a] All currents in units of nanoamperes.

[b] I_D = bulk conduction current
I_R = surface conduction current
I_S = secondary collector current

[c] Steady state.

[d] Not measured.

Table 7. Stored and Drained Charge From IO Coated FEP Teflon

Beam Pot. (kV)	Charge Stored	Charge Leaked
10	1.21×10^{-9} C	0.53×10^{-9} C
15	1.47×10^{-9} C	0.80×10^{-9} C
20	1.89×10^{-9} C	0.84×10^{-9} C

Table 8. Conductive OSR Development Test Matrix

OSR MATERIAL	TILE SIZE	TILE MODIFICATION	TEST SAMPLE SIZE	ADHESIVE	COATING FRONT	COATING BACK	SAMPLE ID #
Fused Silica (Corning 7940)	1" Square	None	3" x 3"	Cond.RTV	--	Ag	#52
" "	4.5" diam	Solid disc	4.5" diam	--	--	--	#46
Microsheet (Corning 0211)	1" Square	None	3" x 3"	Cond.RTV	--	Ag	53
" "	1" "	None	4.5" diam.	Cond.RTV	--	Ag	57
" "	1" "	None	3" x 3"	Cond.RTV	ITO	Ag	86
" "	2 cm "	None	3" x 3"	Sylgard 182	--	Ag	34
" "	2 cm "	None	3" x 3"	Cond.RTV	--	Ag	70
" "	2 cm "	None	3" x 3"	Cond.RTV	ITO	Ag	38
" "	2 cm "	None	3" x 3"	Cond.RTV	GE-1TL frit	Ag	39
" "	2 cm "	Chamfered	3" x 3"	Cond.RTV	--	Ag	71
" "	2 cm "	Chamfered	3" x 3"	Cond.RTV	IO	Ag	72
" "	2 cm "	Chamfered	3" x 3"	Cond.RTV	ITO	Ag	85
GE-1TL	1" "	None	3" x 3"	Cond.RTV	--	Ag	64
" "	4.5" diam	Solid disc	4.5" diam	--	--	--	42
--	--	--	4.5" diam	Cond.RTV	--	--	33

Table 9. Summary of Currents in RTV With Graphite Filler

Beam Potential (kV)	I_D Steady State (nA)	I_S Steady State (nA)	Surface Potential (kV)
2	200	100	.09
4	250	80	.16
6	300	80	.16
8	350	80	.16
10	370	85	.15
15	480	100	.12
20	490	90	.09

Table 10. Summary of Currents of Uncoated Fused Silica Square OSR Mosaic

Beam Potential (kV)	I_D		I_R		I_S	Max. Surface Potential (V)
	Peak (nA)	S.S.[b] (nA)	Peak (nA)	S.S. (nA)	S.S. (nA)	
2	--	31	--	83	295	-400
4	90	38	13	19	290	-2240
6	> 100	50	8	23	275	
10	190	55	8	29	260	
15	> 200	90	--	26	220	

Table 11. Summary of Currents in ITO Coated Microsheet OSR Mosaic

Beam Potential (KV)	I_D		I_S		I_D/I_S
	Peak (nA)	S.S.[b] (nA)	Peak (nA)	S.S. (nA)	S.S.
10	260	200	-	30	6.6
	80	80	31	15	5.3
15	140	110	-	16	6.8
	40	40	7	5	8.0
20	110	80	17	12	6.6

Table 12. Summary of Currents in ITO Coated Chamfered 16 Tile Microsheet (2 cm square) OSR Matrix

Beam Potential (kV)	I_D		I_S		I_R	Surface Potential (V)
	Initial (nA)	S.S (nA)	Initial (nA)	S.S (nA)	S.S (rA)	
2	100	100	100	90	70	0
5	140	180	70	45	25	3
10		200	30	25	15	8
15	230	250	45	40	14	-
20	220	240	35	35	14	12

Table 13. Summary of Current and Surface Potential on GE-1TL OSR Mosaic

Beam Potential (kV)	I_D (nA)	I_S (nA)	$I_D/(I_S+I_D)$	Surface Potential (V)
2	65	550	.10	7
5	270	250	.52	8
10	350	190	.64	9
15	430	210	.67	9
20	450	220	.67	9

Table 14. Average Transmittance for Coated and Uncoated FEP Telfon Under Electron/UV Exposure

Sample	Pre Test Transmittance (%)	Post Test Transmittance (%)
FEP Teflon	90.3	87.0
FEP-Teflon (Heat-treated)	89.5	87.5
FEP/IO (200 MΩ)	84.6	79.6
FEP/IO + CO[a] (2 KMΩ)	35.0	82.0
FEP/IO + CO (200 MΩ)	84.4	81.7
FEP/IO + CO (2 MΩ)	81.8	78.9

[a] CO - Chromium Oxide

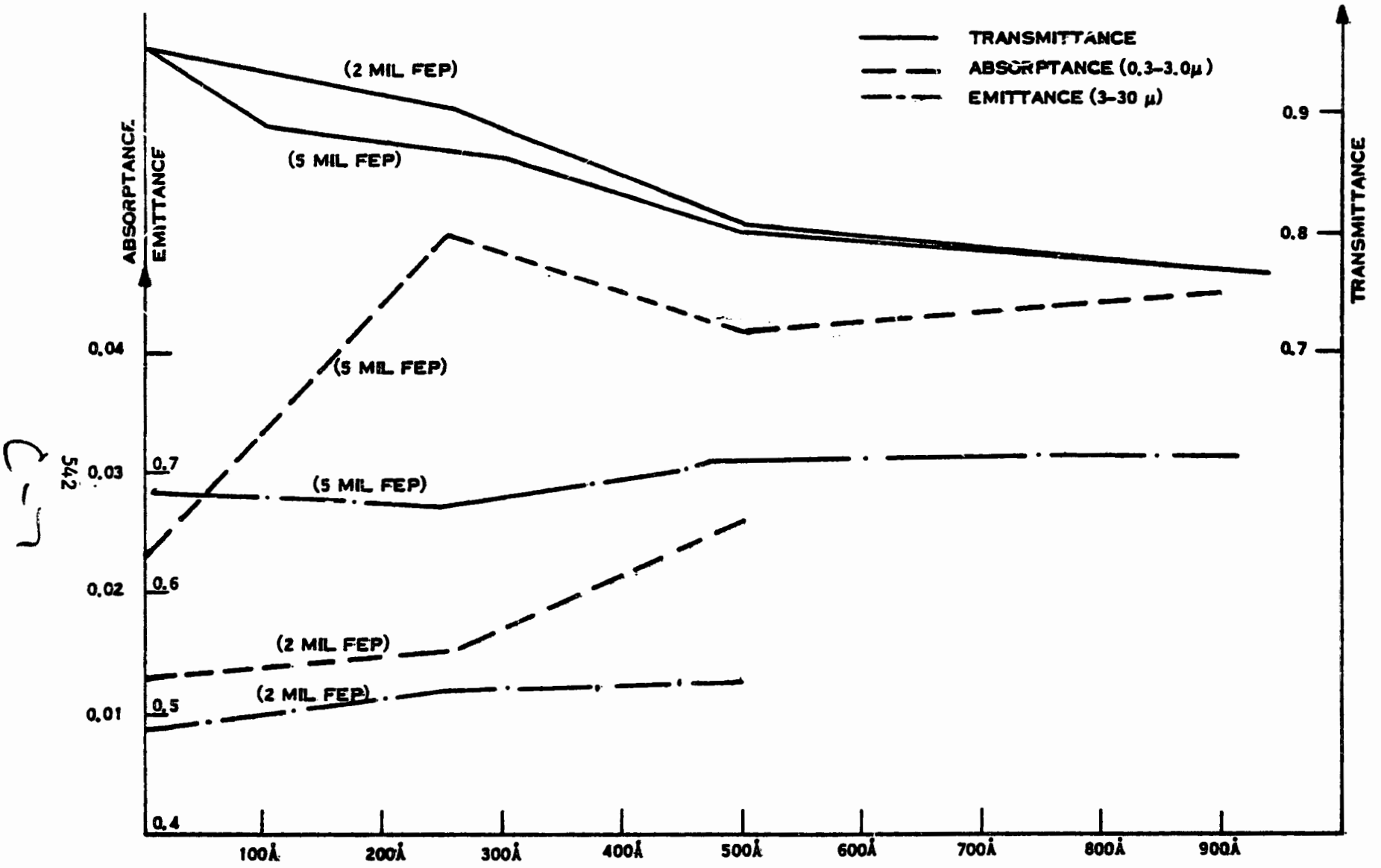

Figure 1. Optical Characterization of ITO Coating Thickness Dependence

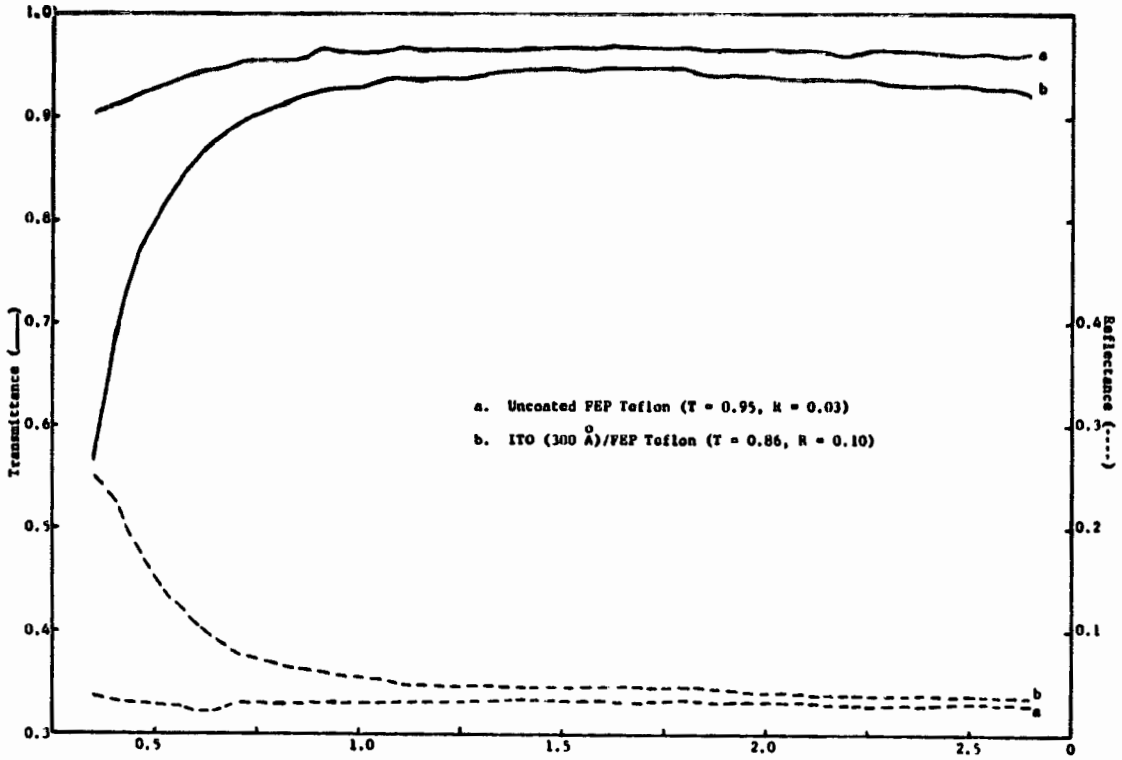

Figure 2a. Transmittance and Reflectance of ITO Coated FEP Teflon

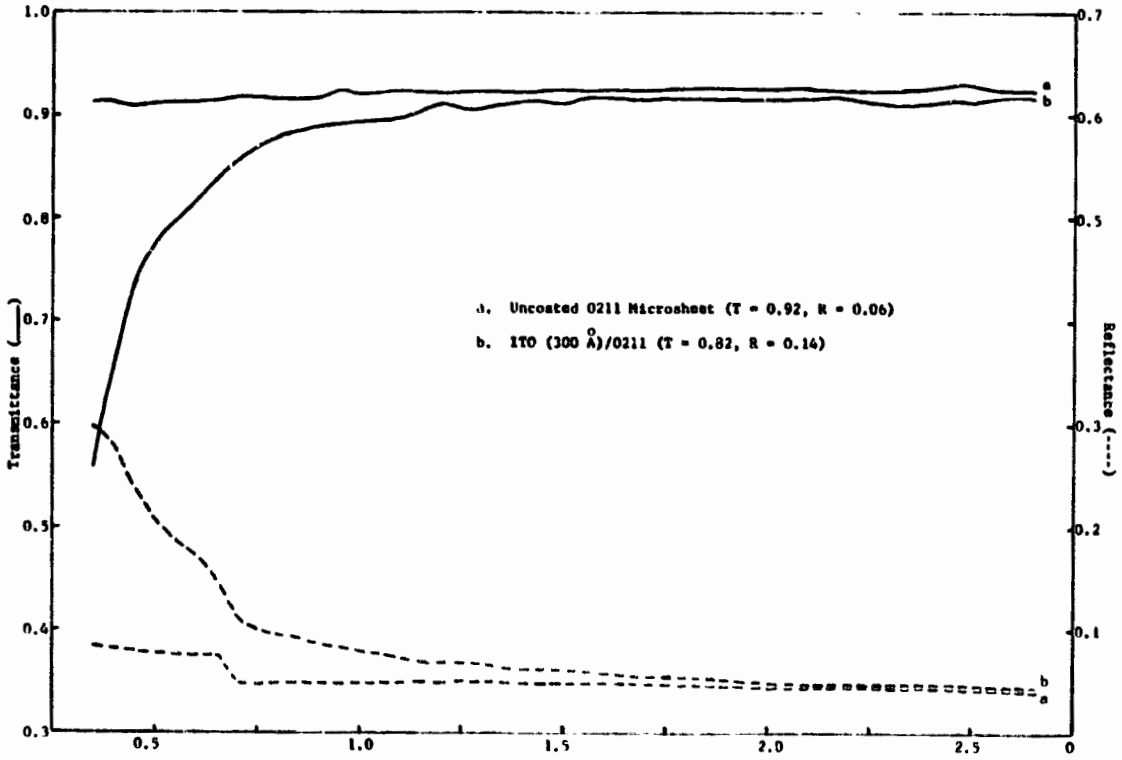

Figure 2b. Transmittance and Reflectance of ITO Coated Microsheet

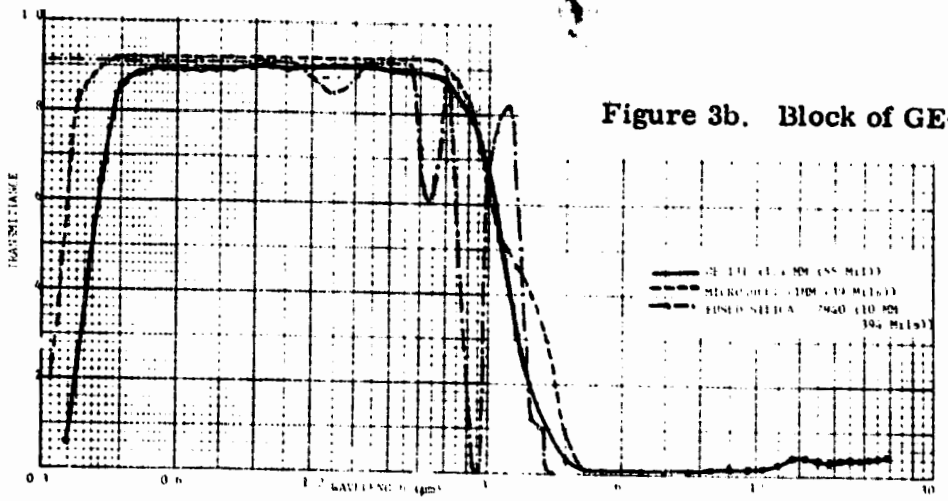

Figure 3b. Block of GE-1TL Glass

Figure 3a. Transmittance of Fused Silica, Borosilicate and GE-1TL Glass

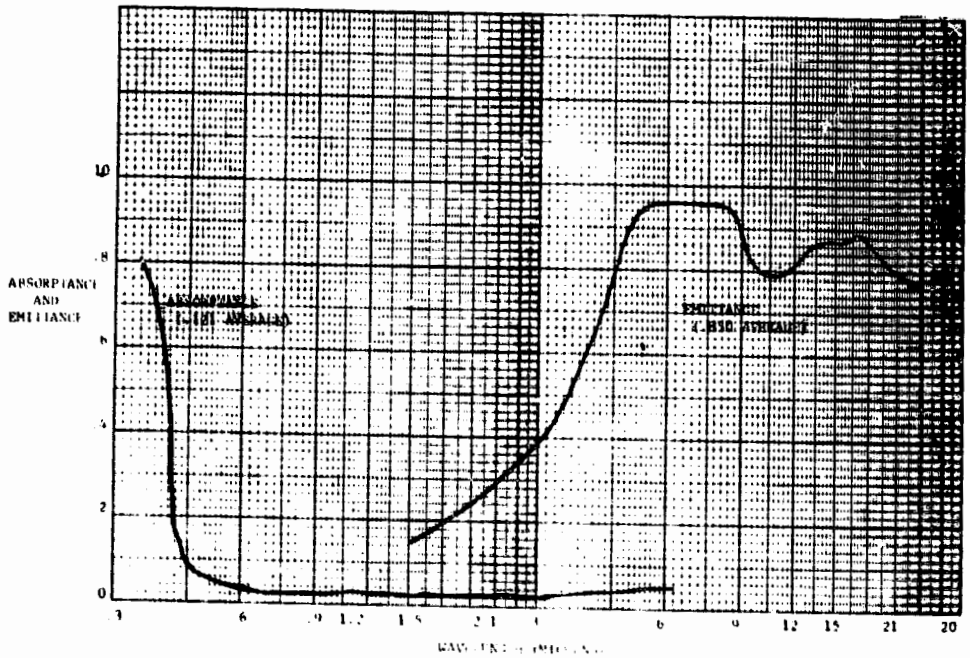

Figure 3c. Solar Absorptance and IR Emittance of GE-1TL Glass (10 Mil)

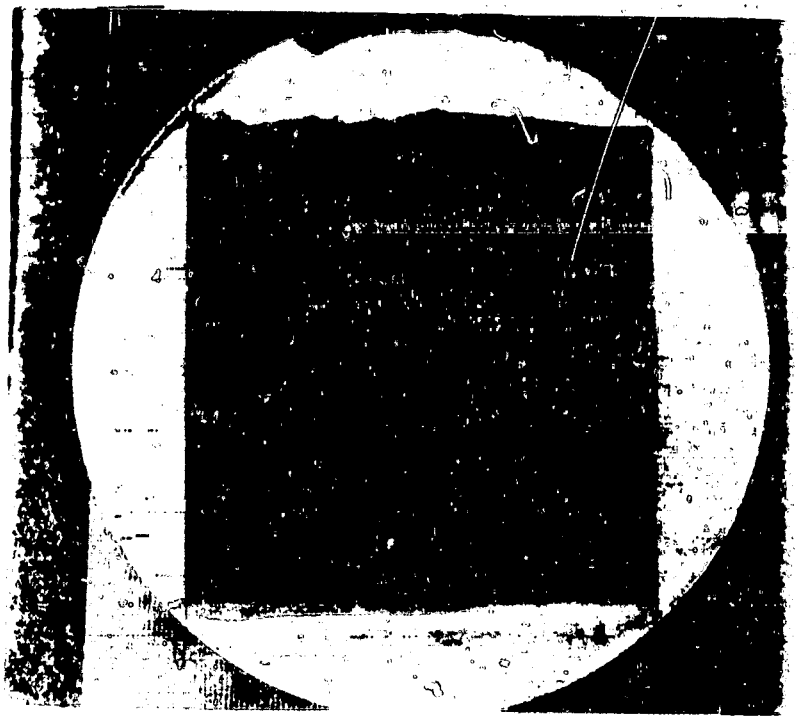

Figure 4a. OSR Configuration of ITO Coated One-Inch Square Microsheet

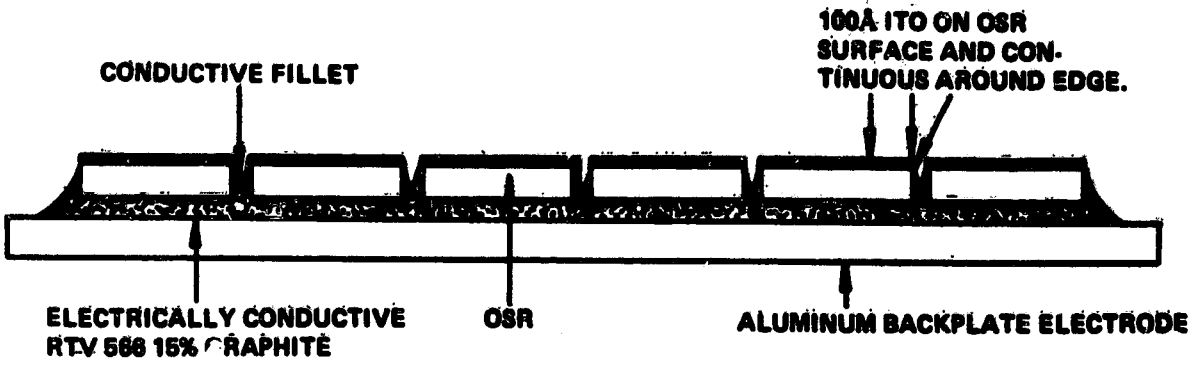

Figure 4b. Continuous Antistatic Grounded OSR Configuration

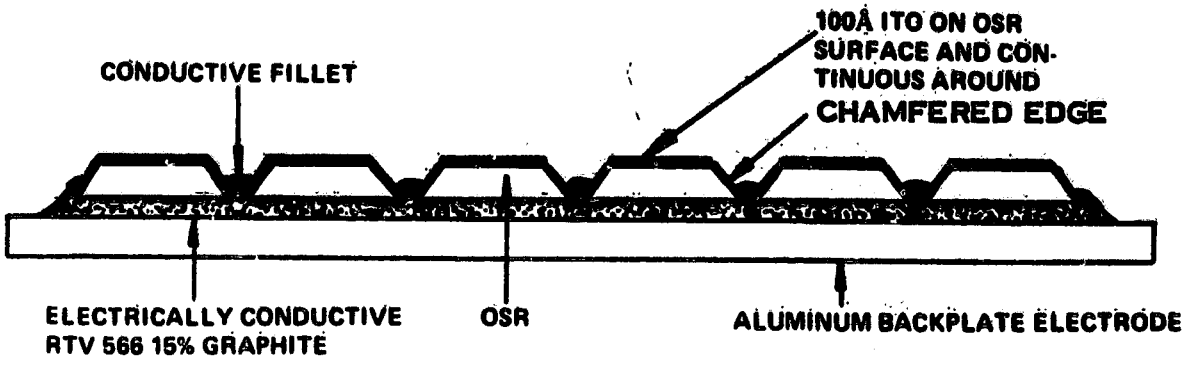

Figure 4c. Continuous Antistatic Grounded Chamfered OSR Configuration

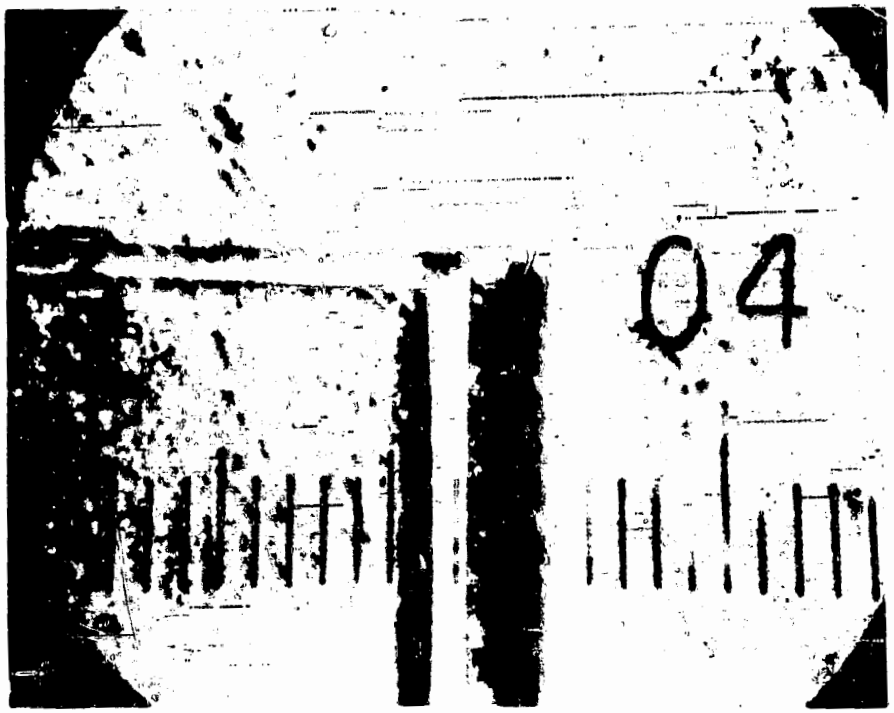

Figure 5a. Chamfered Edges of 10 Mil Thick Fused Silica

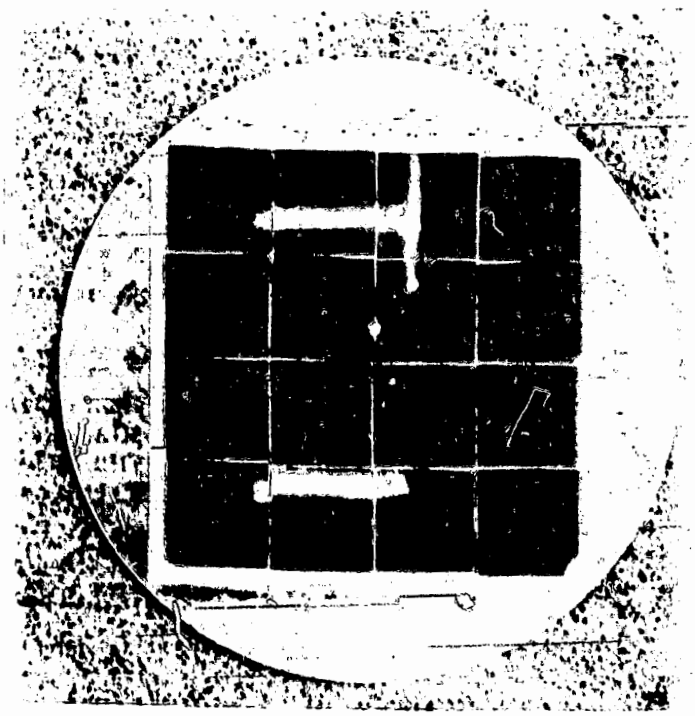

Figure 5b. ITO Coated OSR Matrix of Chamfered 2 cm Square Microsheet

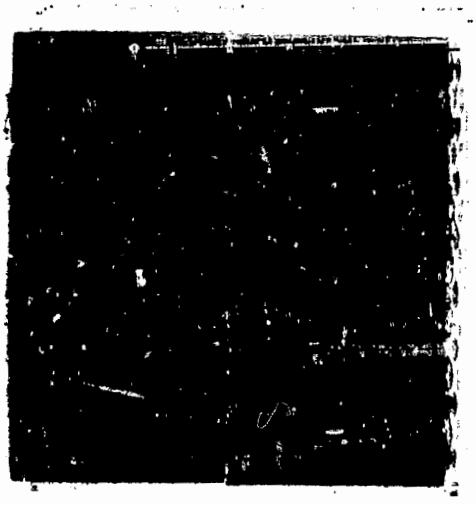

Figure 6. Active Solar Cell Array with Uncoated Microsheet Coverglass

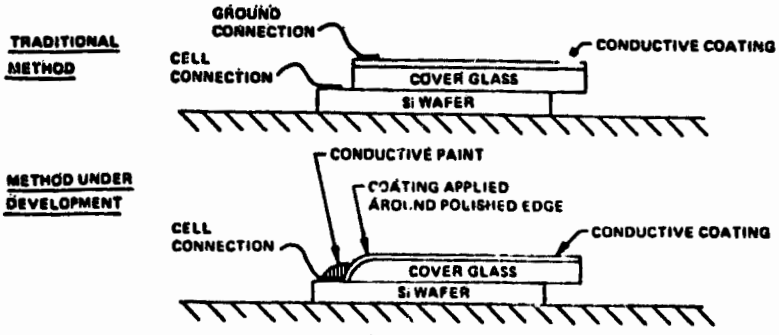

Figure 7a. Grounded Coverglass Design

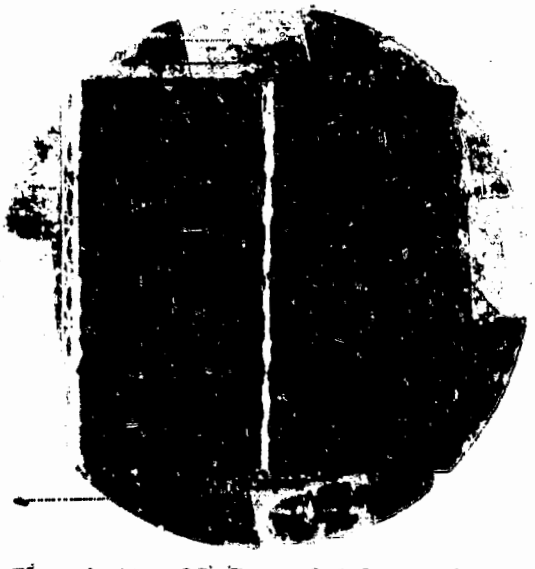

Figure 7b. Active IO Coated Solar Cell Array with 1109S Conductive Epoxy Ground Strip

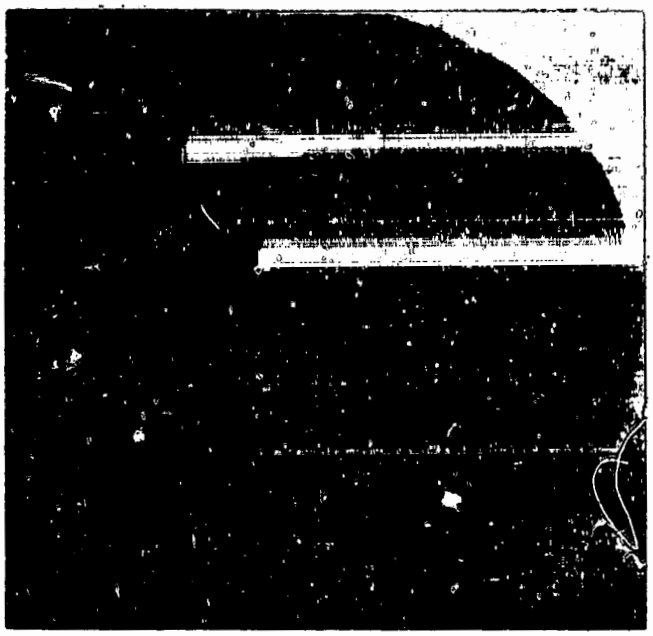

Figure 8. Copper Foil Grounding Connection on Kapton Using Pyralux Adhesive

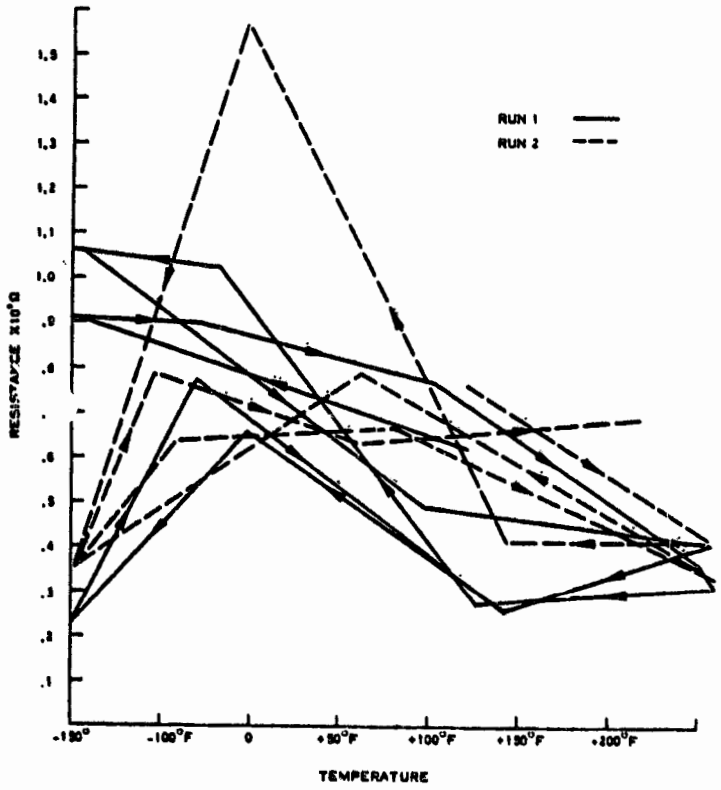

Figure 9. Resistance Cycling of Conductive Copper Tape Ground Strap on ITO and FEP Teflon (10 μA Current)

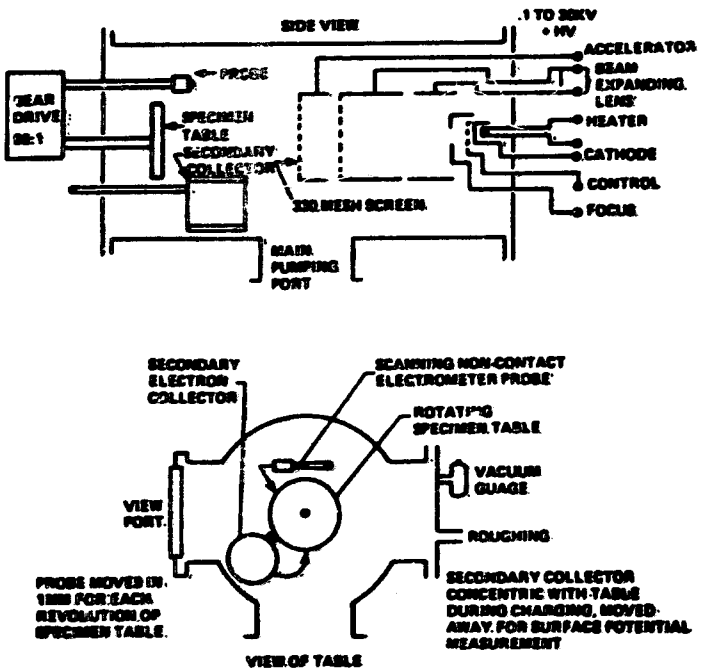

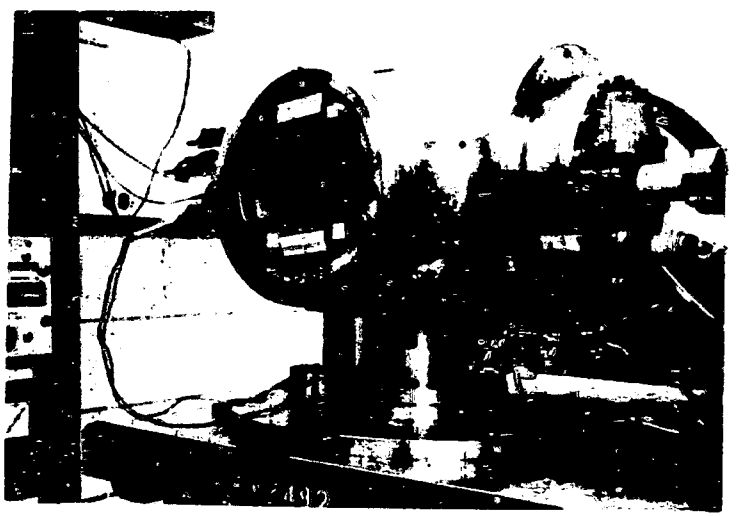

Figure 10. EST Test Facility

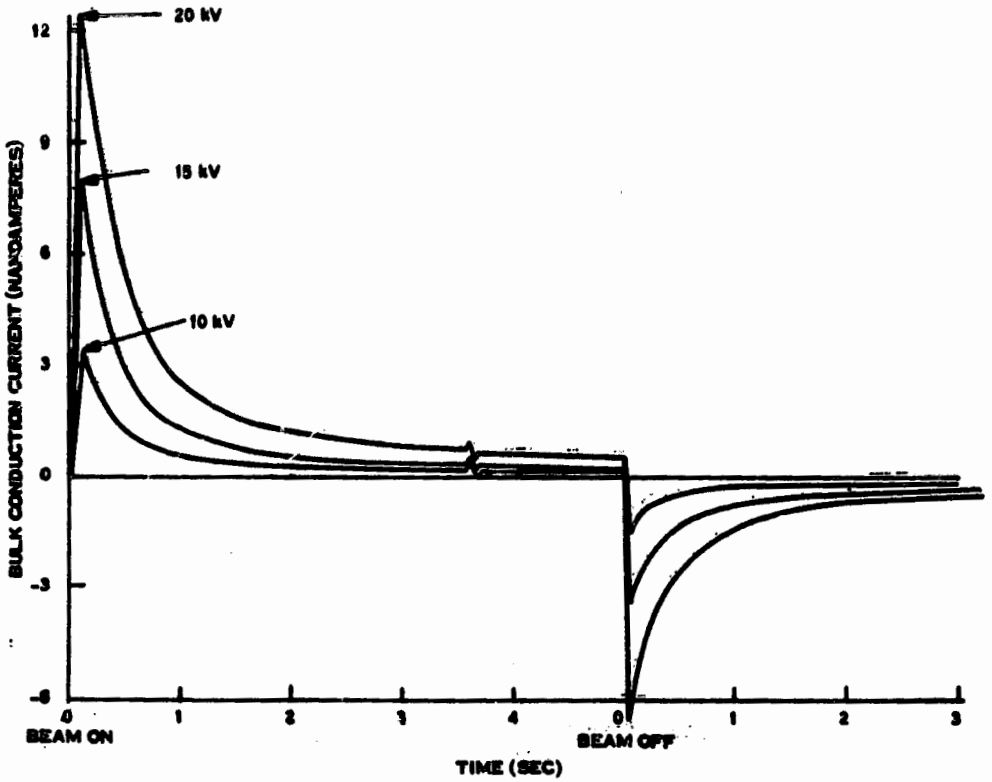

Figure 11. Bulk Conduction Currents for IO Kapton

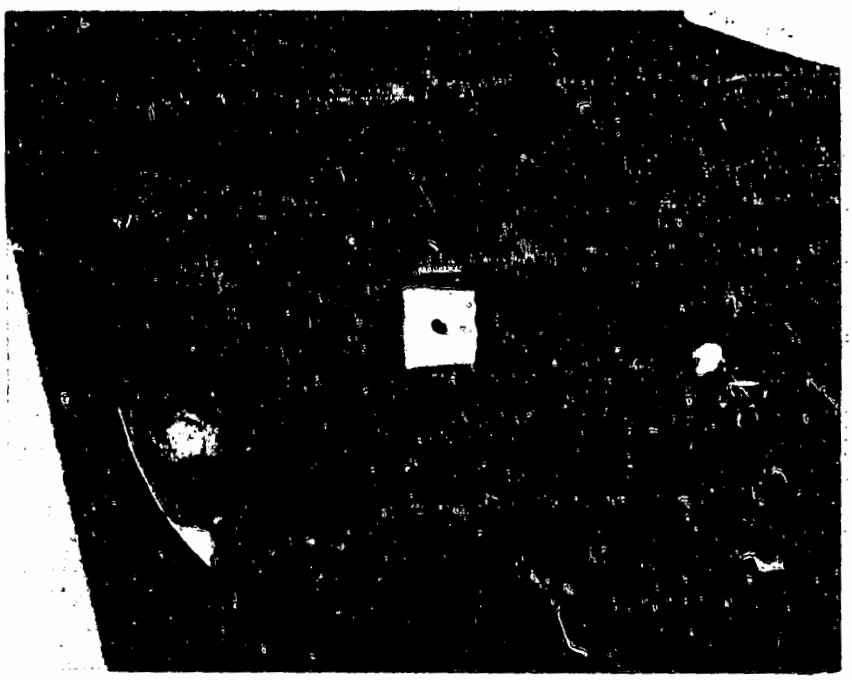

Figure 12a. ESD Test Configuration for Copper Tab Bonded to ITO Coated Kapton with Eccobond 56C

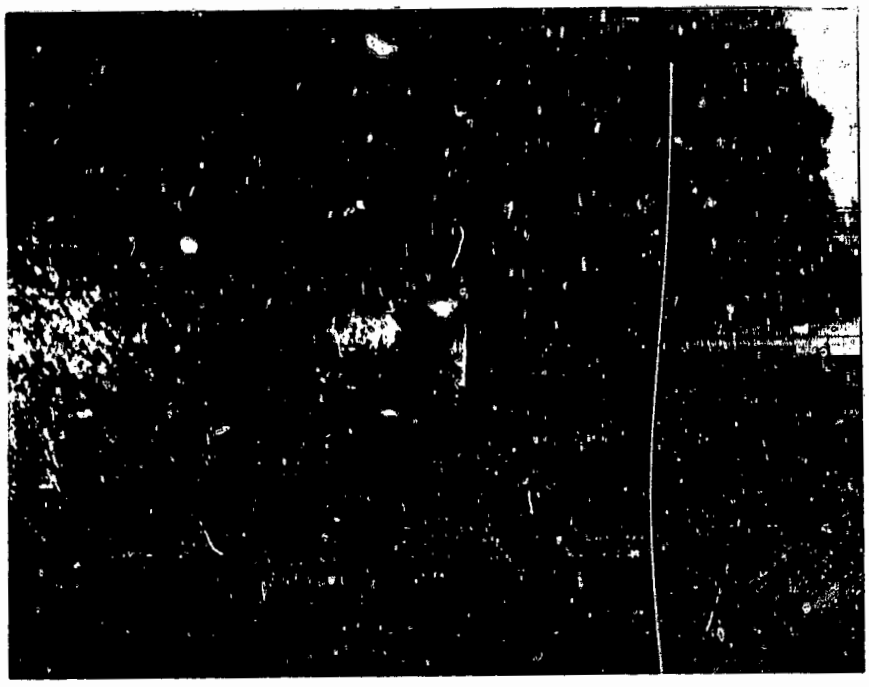

Figure 12b. 1/2" x 1/2" Conductive Copper Tape Ground Bond to ITO Coated FEP Teflon

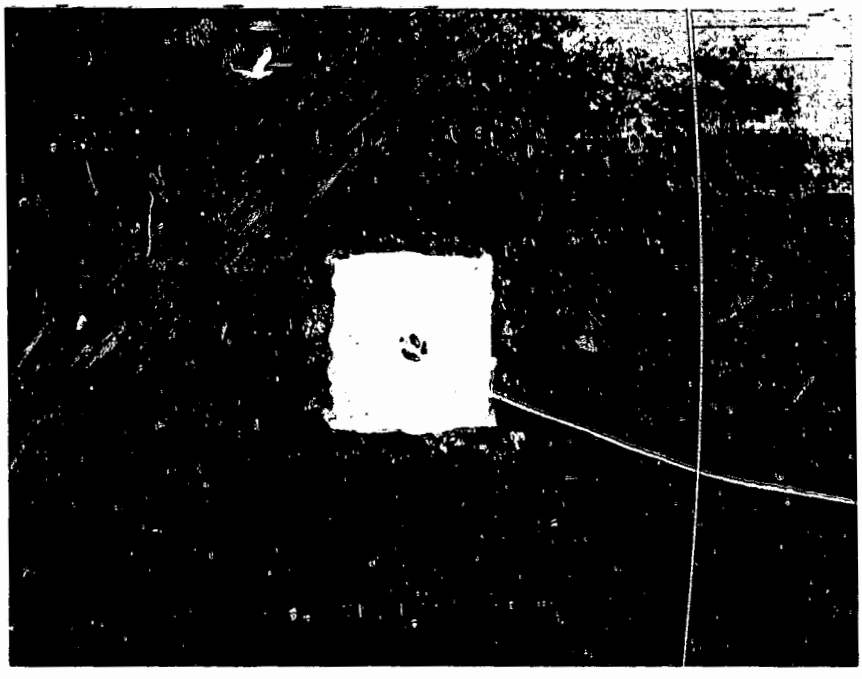

Figure 12c. 1/2" x 1/2" Copper Ground Tab Bonded to ITO Coated FEP Teflon with Eccobond 56C Conductive Cement

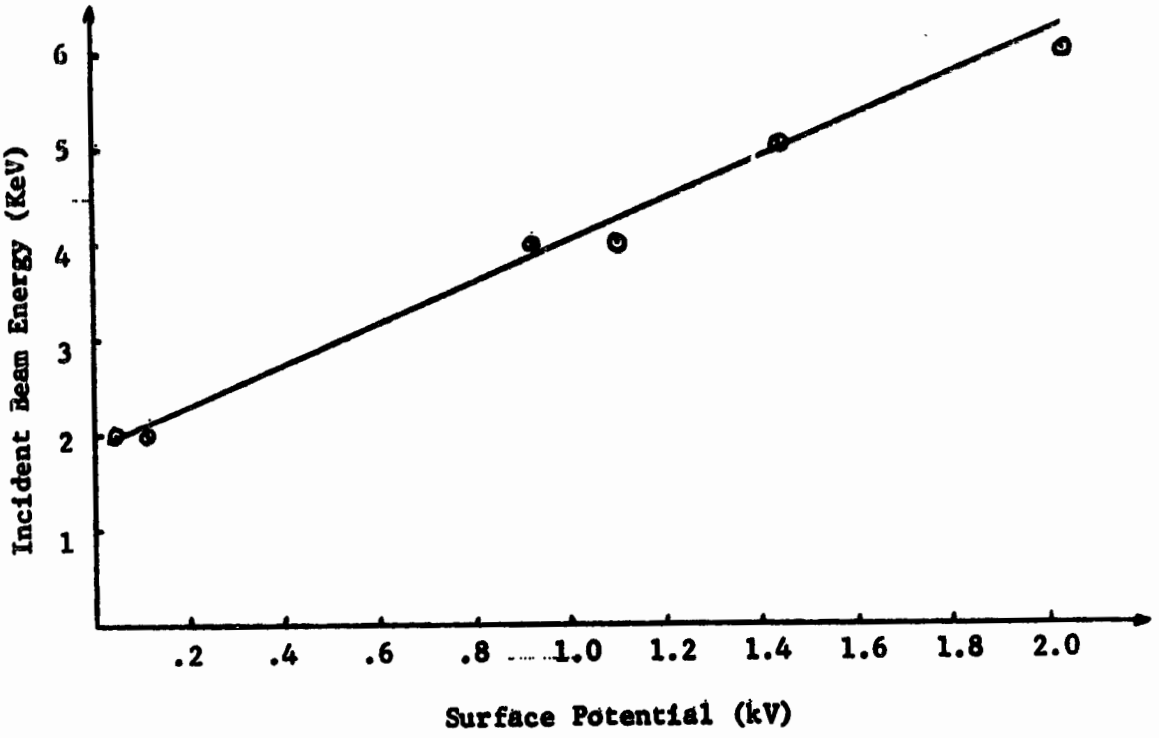

Figure 13. Surface Potential of Uncoated OSR Matrix in Electron Beam

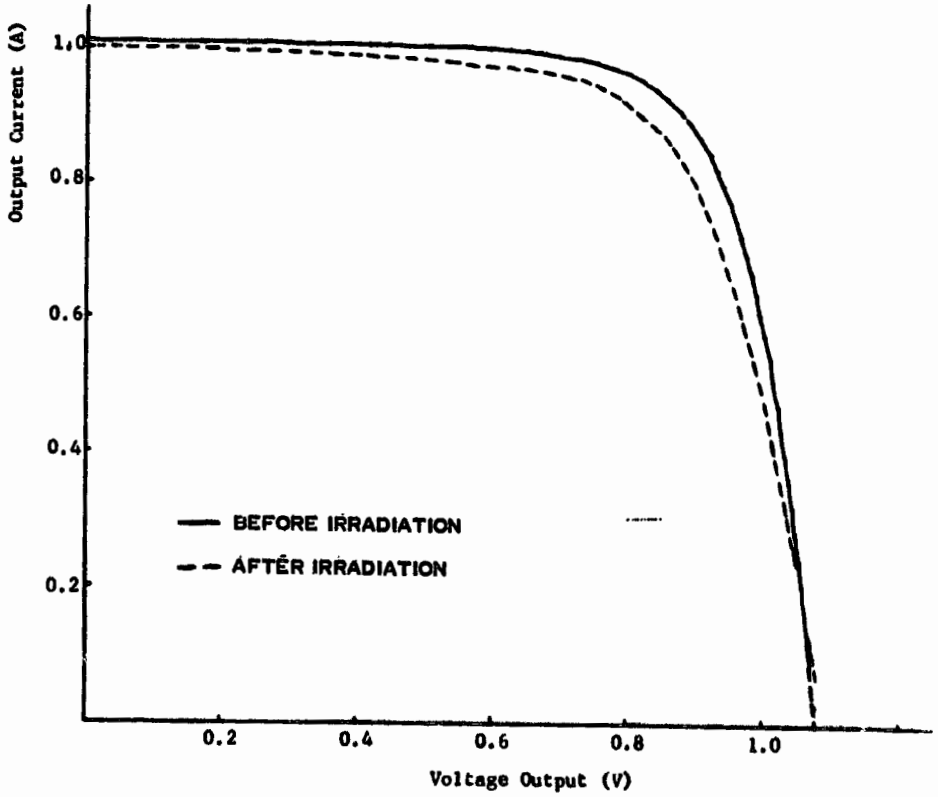

Figure 14. 2 x 4 IO Coated Solar Cell Array Performance After Electron Irradiation

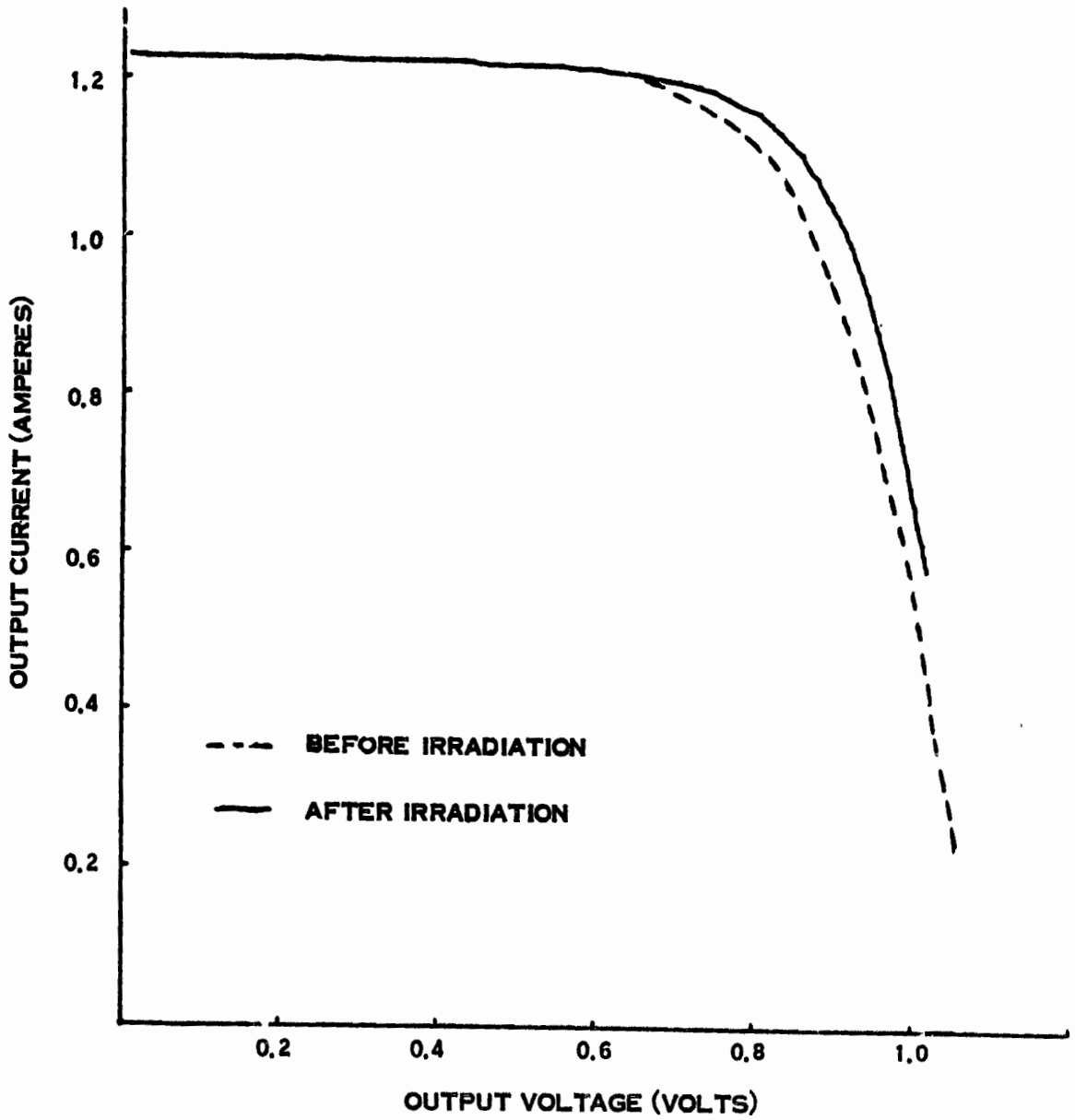

Figure 15. 2 x 4 Array With PPE Glass Without Conductive Coating After Electron Irradiation